AAPT PHYSICS EDUCATION | AMERICAN JOURNAL of PHYSICS

Observing the Maxwell–Boltzmann distribution in LED emission spectra

Jed Brody, Daniel Weiss, and Pearl Young

Citation: Am. J. Phys. **78**, 933 (2010); doi: 10.1119/1.3429980
View online: http://dx.doi.org/10.1119/1.3429980
View Table of Contents: http://ajp.aapt.org/resource/1/AJPIAS/v78/i9
Published by the American Association of Physics Teachers

Observing the Maxwell–Boltzmann distribution in LED emission spectra

Jed Brody, Daniel Weiss, and Pearl Young
Department of Physics, Emory University, Atlanta, Georgia 30322

(Received 20 January 2010; accepted 26 April 2010)

We observe the Maxwell–Boltzmann distribution in the emission spectra of six LEDs spanning the visible spectrum. © *2010 American Association of Physics Teachers.*
[DOI: 10.1119/1.3429980]

I. INTRODUCTION

LEDs are ubiquitous devices that are gaining popularity as illumination sources. Advanced students are likely aware that LEDs are neither blackbodies nor monochromatic sources. Students might wonder whether the spectral content of LED emission can be predicted from fundamental principles. The answer is a qualified yes. The high-energy region of the emission spectrum follows the Maxwell–Boltzmann distribution.[1,2]

Students must be familiar with basic semiconductor concepts before studying LED spectra in depth. There are many excellent online resources, including Ref. 3. Essential concepts include band structure and electron-hole recombination.

LEDs emit light when electrons in the conduction band recombine with holes in the valence band. This basic mechanism is represented in Fig. 1. The conduction band is mostly empty, and the states occupied by electrons are shown as black dots. The valence band is mostly full, and the unoccupied states are known as holes and shown as white dots.

Consider the transition of an electron from energy E_1 in the conduction band to energy E_2 in the valence band. Energy is conserved, and hence a photon with energy $\varepsilon=E_1-E_2$ is released. Momentum is also conserved, and because the photon's momentum is negligibly small, the electron's momentum is conserved during the transition.[4] The rate of recombination, $R(\varepsilon)d\varepsilon$, is proportional to the product of electron concentration, $n(E_1)$, and hole concentration, $p(E_2)$,[4,5]

$$R(\varepsilon)d\varepsilon = P_{12}(E_1,E_2)n(E_1)p(E_2)d\varepsilon, \tag{1}$$

where $P_{12}(E_1,E_2)$ is the probability that a momentum-conserving transition takes place.

To determine the product $n(E_1)p(E_2)$, we must use the density of directly associated states.[4] (If an electron in the conduction band has the same momentum as a hole in the valence band, the electron and hole are said to occupy directly associated states.) Assuming parabolic bands, the relations between energy and momentum are

$$E_1 - E_C = \frac{p_x^2 + p_y^2 + p_z^2}{2m_e^*} \tag{2}$$

and

$$E_V - E_2 = \frac{p_x^2 + p_y^2 + p_z^2}{2m_h^*}, \tag{3}$$

where E_C and E_V are the edges of the conduction and valence bands and m_e^* and m_h^* are the effective masses of electrons and holes. The components of momentum are written explicitly to emphasize that each component must be conserved during a transition.

The sum of Eqs. (2) and (3) yields

$$\varepsilon - E_g = \frac{p_x^2 + p_y^2 + p_z^2}{2m_r}, \tag{4}$$

where $E_g=E_C-E_V$ is the bandgap energy and $m_r=(1/m_e^* + 1/m_h^*)^{-1}$ is the reduced mass.

The density of directly associated states, $N(\varepsilon)$, is found by considering a differential spherical shell in momentum space. The volume of the shell is

$$N(\varepsilon)d\varepsilon \sim (\varepsilon - E_g)^{1/2}d\varepsilon. \tag{5}$$

The carrier concentration is the product of the density of states and the probability that a state is occupied. This probability is given by the Fermi–Dirac distribution, which reduces to an exponential (the Maxwell–Boltzmann distribution) when the quasi-Fermi levels (φ_n and φ_p) are far from the band edges. Thus Eq. (1) can be written as

$$R(\varepsilon)d\varepsilon = P_{12}(E_1,E_2)N(\varepsilon)\exp\left(-\frac{E_1-\varphi_n}{kT}\right) \times \exp\left(-\frac{\varphi_p - E_2}{kT}\right)d\varepsilon. \tag{6}$$

The first exponential term is the probability that a state at energy E_1 is occupied by an electron, and the second exponential term is the probability that a state at energy E_2 is occupied by a hole. We substitute Eq. (5) into Eq. (6) and simplify to find

$$R(\varepsilon)d\varepsilon \sim P_{12}(E_1,E_2)(\varepsilon - E_g)^{1/2}\exp\left(-\frac{\varepsilon}{kT}\right)d\varepsilon. \tag{7}$$

$P_{12}(E_1,E_2)$ in Eq. (6) is determined by use of Fermi's golden rule. After pages of laborious calculations, we arrive at the conclusion that $P_{12}(E_1,E_2)$ is proportional to ε.[6] Accordingly,

$$R(\varepsilon)d\varepsilon = C\varepsilon(\varepsilon - E_g)^{1/2}\exp\left(-\frac{\varepsilon}{kT}\right)d\varepsilon, \tag{8}$$

where C is a constant. The factor of ε is frequently neglected because it varies only slightly over the width of the emission spectrum.[1,6,7]

Measured LED spectra tend to be more symmetrical than predicted by this simple model.[5] A significant departure from this model is due to sub-bandgap recombination,[4] which affects only the low-energy side of the spectrum. Because Eq. (8) does not give the correct energy dependence on the low-energy side, we do not expect Eq. (8) to fit measured results at low energies.

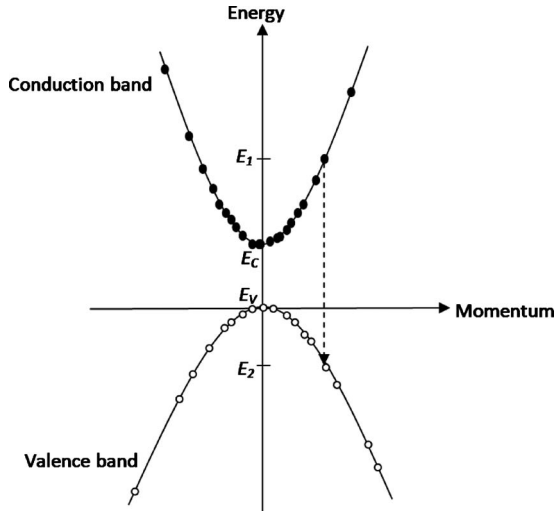

Fig. 1. Recombination of an electron at energy E_1 and a hole at energy E_2. Their momenta are identical.

We can fit the high-energy side of our measured results because high energies are dominated by the exponential term and unaffected by the low-energy complications. The high-energy regions of LED emission spectra are thus manifestations of the Maxwell–Boltzmann distribution. Accordingly, we expect the high-energy regions of LED spectra to fit the form $A[\exp(-\varepsilon/kT)]$, where A is a constant independent of T.

A more accurate algorithm was recently established for determining LED temperatures from emission spectra.[1] This algorithm recognizes that the factor of $(\varepsilon-E_g)^{1/2}$ in Eq. (8) causes the high-energy tail to deviate slightly from a true exponential. We now follow the discussion in Ref. 1, filling in some steps. We first derive $\partial(\ln R)/\partial\varepsilon$ from Eq. (8), obtaining

$$\frac{\partial \ln(R)}{\partial \varepsilon} = \frac{1}{2(\varepsilon - E_g)} - \frac{1}{kT} \tag{9}$$

if the factor of ε in Eq. (8) is neglected. If we apply elementary calculus to Eq. (8) and neglect the factor of ε, we find that the energy of peak emission is $E_P=E_g+kT/2$. We will evaluate the derivative in Eq. (9) at the energy $\varepsilon=E_P+\Delta$ so that $\varepsilon-E_g=kT/2+\Delta$. We substitute this form of ε is into Eq. (9) and solve for T to find

$$T = \frac{\Delta}{k}\left(\sqrt{1 - \frac{2}{\left.\frac{\partial \ln R}{\partial \varepsilon}\right|_{E_P+\Delta} \times \Delta}} - 1 \right). \tag{10}$$

Ideally, the temperature determined by Eq. (10) is the same for all Δ where data exist. However, the spectrum at very high energies ($\Delta>0.15$ eV) is distorted by absorption in the window material surrounding the junction, and the spectrum near the peak ($\Delta<0.09$ eV) may be distorted by electron-phonon interactions and other complicated phenomena.[1] Therefore, we will look in the range of $0.09\ \text{eV}<\Delta<0.15$ eV. To estimate $\partial(\ln R)/\partial\varepsilon$ from our data, we determine the slope of $\ln R$ versus ε, using the 31 data points closest to $E_P+\Delta$.[1]

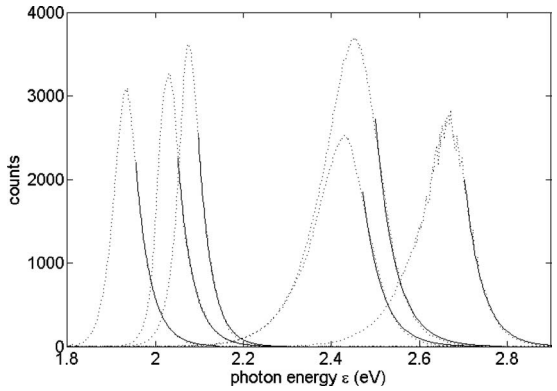

Fig. 2. Measured data (dotted lines) and exponential fits (solid lines) for six LEDs. From left to right, the curves correspond to red, orange, yellow, green, aqua, and blue LEDs.

II. EXPERIMENT

Six LEDs (red, orange, yellow, green, aqua, and blue) were obtained from Super Bright LEDs.[8] A homemade current source[9] was used to supply a stable current of 6.6 mA to each LED. Light from each LED was directed into an Ocean Optics USB2000 spectrometer, which is a 2048-pixel CCD-detector array. We took ten measurements of each LED spectrum using a 50 ms acquisition time for each measurement. We averaged each set of ten measurements to obtain our final results, which are shown in Fig. 2.

We fit the high-energy region of each spectrum to $A[\exp(-\varepsilon/kT)]$ using A and T as fitting parameters for each spectrum. The high-energy regions of the six spectra nicely match these exponential fits. (The smaller the fitting range, the more perfect the fit. We arbitrarily extended the fit up to a value of 71% of the peak.) We expect T to be somewhat higher than the ambient temperature because the active region of the LED heats up during operation. That is, T is the temperature of the p-n junction, not the ambient temperature. We find temperatures of 387, 396, 343, 505, 530, and 466 K for the red, orange, yellow, aqua, green, and blue LEDs, respectively.

Although the fits appear excellent, serious errors in our estimates of the temperature arise from the slight deviations of the high-energy regions from exponential decay. We can use Eq. (10) to increase the accuracy of our temperature estimates. The resulting values of T vary by less than 10% over all Δ from 0.09 to 0.15 eV. The results for the red, orange, yellow, green, aqua, and blue LEDs were 285–315, 314–335, 254–289, 363–384, 396–413, and 359–368 K, respectively. In all cases, these temperatures are lower than our initial, less sophisticated estimates. These lower temperatures are also more reasonable, considering that the highest recommended temperature for our LED junctions is 358 K.[8] To further improve our estimates of junction temperature, we would have to calibrate our results with temperatures obtained some other way.[1]

Students can recognize the importance of further refinement of the physical model because Eq. (8) predicts a relatively abrupt rise in the low-energy region of each spectrum, which is not observed experimentally.[5]

Another interesting problem is to estimate the bandgap energy, which ideally is the lowest possible photon energy. We can determine the lowest photon energy by finding where

the measured results fall to zero on the left side. We find energies of 1.79, 1.88, 1.92, 1.91, 2.04, and 2.22 eV for red, orange, yellow, green, aqua, and blue LEDs, respectively. We observe that the green, aqua, and blue LEDs have very long low-energy tails. These tails may indicate sub-bandgap recombination. The real bandgap energies may be higher than our estimates.

Bandgap energy may be a new concept for students. Therefore, it may be valuable for students to relate the quantitative data to the simple concept of visible color. The peak of the emission spectrum is closely related to the color perceived by the eye. We find emission peaks at 640, 611, 598, 511, 505, and 464 nm for the red, orange, yellow, green, aqua, and blue LEDs, respectively. These wavelengths correspond well with the colors observed.

III. DISCUSSION

We observed the Maxwell–Boltzmann distribution in the emission spectra of six LEDs spanning the visible spectrum. Although the associated theory is advanced, two undergraduate students (authors Weiss and Young) were able to collect all the data, learn a great deal about unfamiliar topics, and improve upon the instructions they were given.

ACKNOWLEDGMENTS

The authors gratefully acknowledge Keith Berland for his expert guidance and Gary Hunter for his assistance with software. The authors thank the anonymous reviewers for suggesting many significant improvements.

[1] Z. Vaitonis, P. Vitta, and A. Žukauskas, "Measurement of the junction temperature in high-power light-emitting diodes from the high-energy wing of the electroluminescence band," J. Appl. Phys. **103**, 093110-1–7 (2008).

[2] Y. Wang *et al.*, "Determination of junction temperature of GaN-based light emitting diodes by electroluminescence and micro-Raman spectroscopy," in CS MANTECH Conference, Tampa, Florida, May 18–21, 2009.

[3] Christiana Honsberg and Stuart Bowden, *Photovoltaics CDROM*, Chap. 3, ⟨pvcdrom.pveducation.org/⟩.

[4] J. I. Pankove, *Optical Processes in Semiconductors* (Dover, New York, 1975), pp. 10, 35–36, 107.

[5] S. O. Kasap, *Principles of Electronic Materials and Devices*, 3rd ed. (McGraw-Hill, New York, 2005), pp. 548–550.

[6] P. Bhattacharya, *Semiconductor Optoelectronic Devices* (Prentice-Hall, Englewood Cliffs, NJ, 1994), p. 219.

[7] E. Rosencher and B. Vinter, *Optoelectronics* (Cambridge U. P., Cambridge, 2002), p. 619.

[8] See: ⟨www.superbrightleds.com/⟩.

[9] T. C. Hayes and P. Horowitz, *Student Manual for the Art of Electronics* (Cambridge U. P., Cambridge, 1989), p. 180.

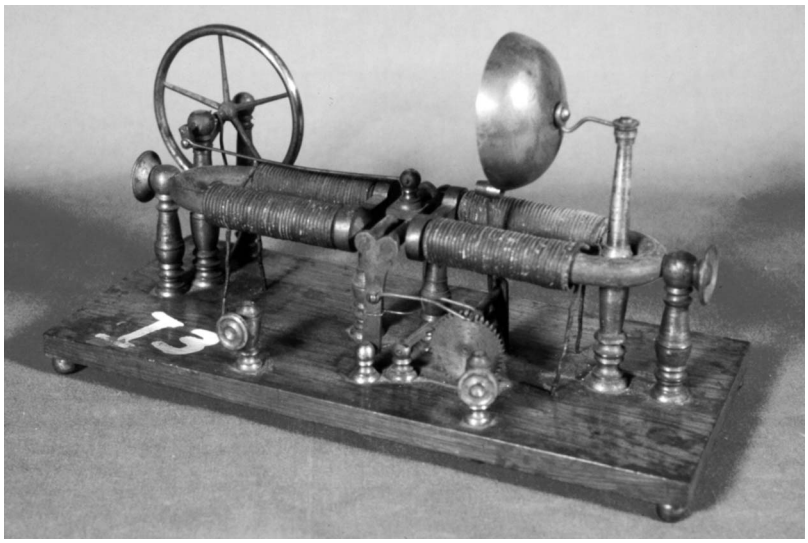

Reciprocating Bell Engine. If you were designing an electric engine in the 1840s you would certainly follow the model of the steam engine. This reciprocating engine is the analogue of the double-acting steam engine in which steam is applied alternately to both sides of the piston. Here the two electromagnets are energized alternately by make-and-break contacts and pull the iron bars between them back and forth. This oscillation motion is converted to rotary motion by the crank mechanism, invented by James Watt. The bell is rung every time the toothed gear, pushed one tooth forward at each oscillation, makes one revolution. This engine is in the apparatus collection of the Wesleyan University in Middletown, Connecticut. It appears in the 1842 edition of Daniel Davis's Manual of Magnetism at $20.00. (Photograph and Notes by Thomas B. Greenslade, Jr., Kenyon College)